Revista Mexicana de Física S **58** (2) 8–11 DICIEMBRE 2012

Magnetic properties of nanowire arrays

R. Lavín[a,b], J.C. Denardin[a], and A. Cortés[c]
[a]*Departmento de Física, Universidad de Santiago de Chile,*
Av. Ecuador 3493, Santiago, Chile,
e-mail: lavin.roberto@gmail.com
[b]*Faculad de Ingeniería, Universidad Diego Portales,*
Ejército 441, Santiago, Chile.
[c]*Departamento de Física, Universidad Técnica Federico Santa María,*
Av. España 1680, Valparaíso, Chile.

Recibido el 25 de junio de 2010; aceptado el 6 de octubre de 2010

This paper shows a general study of the magnetic properties of Ni nanowire arrays; specifically the influence of the electrodeposition potential, length, diameter, and the magnetostatic interaction between nanowires electrodeposited in alumina membranes. The behavior of the coercivity as a function of the length and diameter of the nanowires is explained through an analytical model. Additionally, the magnetic properties as function of the temperature in Ni and the hysteresis curves of segmented Ni/Co nanowires are presented.

Keywords: Nanowires; magnetic properties; magnetic anisotropy; coercivity.

Este artículo muestra un estudio general sobre las propiedades magnéticas de arreglos de nanohilos de Ni; específicamente la influencia del potencial de electrodeposición, longitud, diámetro, y la interacción magnetostática entre nanohilos electrodepositados en membranas de alumina. El comportamiento de la coercividad en función de la longitud y diámetro de los nanohilos es explicado a través de un modelo analítico. Adicionalmente son presentadas las propiedades magnéticas en función de la temperatura en nanohilos de Ni y las curvas de histéresis de nanohilos multisegmentados de Ni/Co.

Descriptores: Nanohilos; propiedades magnéticas; anisotropía magnética; coercividad.

PACS: 75.30.Cr; 75.75.Cd; 81.07.De

1. Introduction

The study of magnetic nanostructured systems is a topic that attracted considerable interest due to their interesting physical properties and potential technological applications [1-3]. In particular, highly ordered arrays of magnetic nanowires produced inside the pores of anodic alumina membranes [4] by electrochemical deposition have been the focus of intense research [5-7]. Different groups have investigated the stable magnetic configurations in function on the aspect ratio of the magnetic cylinders [8,9], the reversion mechanisms of the magnetization in nanowires [10,11], the influence of magnetostatic interactions among nanowires [12-14], and in general, the behavior of the magnetic properties in function of different parameters [15-16]. This paper shows the influence of the electrodeposition potential, length, diameter and temperature of the nanowires on the magnetic properties.

2. Experimental setup

Hexagonal arrays of Ni nanowires of diameters d= $2R$= 50 and 60 nm and different lengths have been prepared by electrodeposition into nanopores of alumina membranes with interpore distance D= 100 nm [12] (see Fig. 1). The electrodeposition of nanowires was performed at different potentials of V = -0.9, -1.0, and -1.1 v. The morphology of the individual nanowires after the dissolution of the alumina was studied by means of scanning electron microscopy (SEM) with a JEOL 5900 LV and transmission electron microscopy using a JEOL 2010F, checking the high ordering of the hexagonal arrays and the large aspect ratio of the nanowires [12]. The chemical characterization of the nanowires was made by means of energy-dispersive analysis of X-rays [12] and X-ray diffraction [17]. The magnetization measurements were performed with a vibrating sample magnetometer and measurements at low temperatures were performed in a Quantum Design MPMS system.

3. Results and disccussion

3.1. Ni nanowire arrays

In this section it is studied the influence of the electrodeposition potential, length and diameter of nanowires on the magnetic properties of Ni nanowire arrays. Figure 2 shows the hysteresis loops with the external field, H, parallel and perpendicular to the nanowires axis, for samples with length L=1 and 4 μm, diameter d=$2R$=50 nm, and lattice constant D=100 nm, as function of the electrodeposition potential V. The difference between the parallel and perpendicular hysteresis loops defines the uniaxial anisotropy; the coercivity and remanence in the parallel configuration are larger than in the perpendicular configuration, indicating that the magnetic easy axis is along the nanowire axis. The magnetic behavior of magnetic nanowire arrays is strongly dependent on the magnetic anisotropies (mainly the shape and crystalline

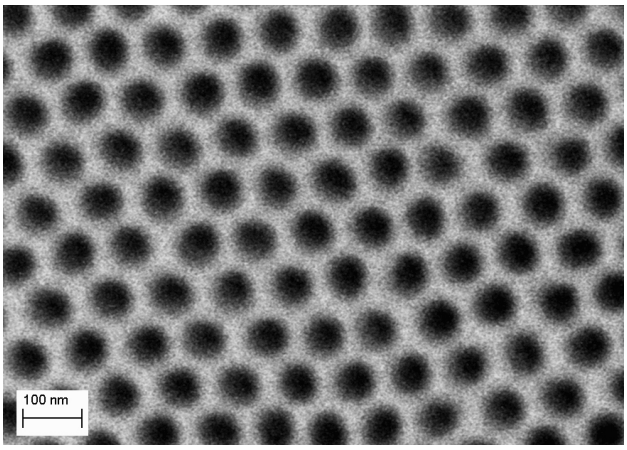

FIGURE 1. SEM image of surface of alumina membrane produced after the two anodization process.

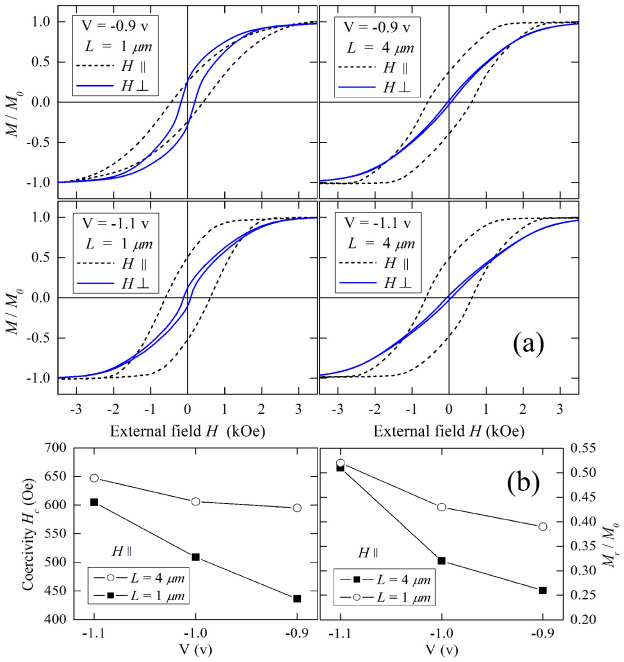

FIGURE 2. (a) Hysteresis loops of Ni nanowire arrays with d=2R=50 nm and lattice constant D = 100 nm at different lengths, L, and electrodeposition potentials, V. (b) Coercivity and remanence as a function of the electrodeposition potential.

anisotropy) and the dipolar interaction between nanowires [16]. In nanowires with a large aspect ratio (L/d) the shape anisotropy will induce a magnetic easy axis parallel to the nanowire axis, and it is expected that the easy axis will lie along the nanowire axis, as can be observed in Fig. 2(a) (except at V = -0.9 v and L = 1 μm).

For the array with length L = 1 μm the coercivity measured (with H||) at the electrodeposition potentials V = -0.9 and -1.1 v changes from 605 Oe to 436 Oe respectively, while for L = 4 μm changes from 647 to 595 Oe respectively. Coercivity values show different variations with the potential for two lengths, due to different aspect ratio of the nanowires. Figure 2(b) shows the coercivity and remanence in function of electrodeposition potential when the external field is applied parallel to the nanowire axis for the samples of the Fig. 2(a).

The effective magnetic anisotropy of the nanowire arrays is determined by four contributions: (i) the shape anisotropy, which will induce a magnetic easy axis parallel to the nanowire axis, (ii) the dipolar interaction between nanowires, which will induce a magnetic easy axis parallel/perpendicular to the Ni/Co nanowire axis, (iii) the crystalline anisotropy and (iv) the magnetoelastic anisotropy, due to stress between the template and the nanowires, which will induce a magnetic easy axis parallel or perpendicular to the stress direction. In Ni and Co nanowires the contribution of the magnetoelastic anisotropy at ambient temperature is negligible compared to other anisotropy terms [18,19]. Thus, the effective anisotropic field of a nanowire array is $H_{\rm eff}$=H_s+H_i+$H_{\rm cris}$, where the first term is the shape anisotropy field, the second term is the dipolar field acting on one nanowire due to all other nanowires in the array, and the third term is the crystalline anisotropy field, that is dependent on the growth conditions of the nanowires [17]. In reference [17] shows that Ni nanowires grown at V = -0.9 v, present only the diffraction peak corresponding to the (111) plane, indicating that the growth axis of the nanowires is along the [111] direction, while at V = -1.1 v, Ni nanowires have a preferred orientation along the [110] direction, and at intermediate potential, V = -0.9 v, X-ray diffraction patterns showed the presence of both, (111) and (110) diffractions peaks. Therefore, the contribution of the crystalline anisotropy field is a function of the electrodeposition potential, as can be observed in Fig. 2(b). In summary, the growth axis of the nanowires depends of the electrodeposition potential, and the crystalline anisotropy depends of the growth axis of the nanowires. Thus, samples of the Ni nanowire arrays grown at different electrodeposition potentials will have different crystalline anisotropy. This is the phenomenon responsible by the dependence of the magnetic properties (coercivity and remanence) as function of the potential.

3.1.1. *Geometry dependence and interaction in Ni nanowire arrays*

The magnetization reversal in a magnetic nanowire, that is, the change in the magnetization from one of its minima -$M_0\hat{z}$ to the other +$M_0\hat{z}$ may occur by means of three main idealized modes of magnetization reversal process that have been identified depending on the geometry and the composition of the wires [20-23]. These modes are known as the *coherent rotation*, with all the spins rotating simultaneously; *transverse wall*, in which spins invert progressively via propagation of a transverse domain wall; and the *vortex wall*, in which spins invert progressively via propagation of a vortex domain wall. In a previous work [12] we have calculated the stray field produced by the array on one nanowire when the reversion of magnetization occurs in transverse mode, which occurs for nanowires with large aspect ratio (L/d) [22]. The coercive

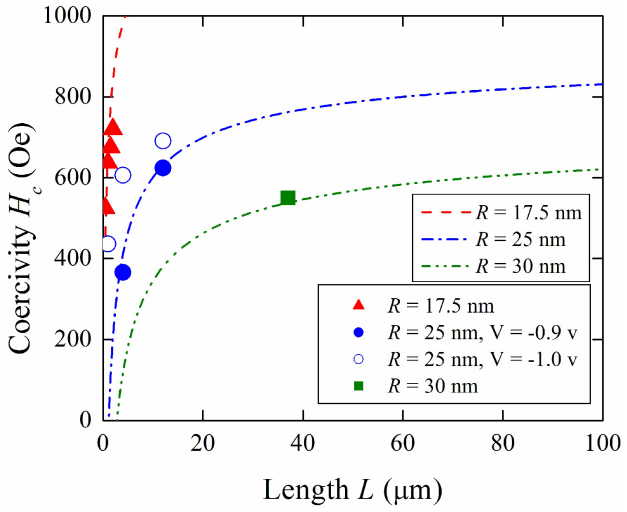

FIGURE 3. (Dash lines) Calculated coercivity obtained from analytical model as a function of the length of the Ni nanowire arrays (for different radii of nanowires), and (dots) coercivities experimentally measured; the triangular dots corresponds to the data taken from [24], and the others dots corresponds to measured data.

field in this case is given by $H_c = H_s - H_{\text{int}}$ [12] where H_{int} corresponds to the stray field induced within the array and given by $H_{\text{int}} = [2K(L)/\mu_0 M_0][\varepsilon|E_{\text{int}}|/\text{K}(L)]^{1/2}$ with K(L) the shape anisotropy constant and E_{int} the interaction field between two nanowires [12]. Figure 3 shows (dash lines) the coercivity calculated as a function of the length of the nanowires for tree different diameters. In this Figure the blue and green dots illustrate the coercive fields measured, and the triangular dots illustrate the coercive fields taken from [24]. Using this approach, the coercivity calculated in function of the length for different diameters gives coercivity values more close to the ones observed in the experimental points, as can be observed in Fig. 3. Also it is important to point out that in this model we have not considered any kind of crystalline anisotropy, which is present in the samples, depending on the electrodeposition conditions. The addition of the crystalline anisotropy (dependent of V) does not modify qualitatively the results, and its effect is equivalent to changing the aspect ratio of the nanowires, as can be observed in Fig. 3 (circular dots) for nanowires with diameter $d = 2R$=50 nm.

3.1.2. Anisotropy and temperature

Figure 4 shows the temperature dependence of the coercivity for Ni nanowires arrays with lengths of L = 4 μm and L=12 μm, measured parallel and perpendicular to the wire axis. For both arrays the coercivity measured parallel to the nanowires increases with the temperature and the coercivity measured perpendicular slightly decreases when the temperature increases. Coercivity values show different variations with the temperature for two lengths. In order to explain these different dependences in Ni one has to consider the contribution of the magnetocrystalline and magnetoelastic anisotropies. The crystalline anisotropy constant of Ni increases two orders of magnitude when temperature decreases from 300 to 5 K. The magnetoelastic anisotropy, on the other hand, depends on the stress applied to the nanowires by the alumina matrix and is affected by the different thermal expansion coefficients of the alumina porous and the nanowires [18]. A more systematic characterization of nanowire arrays measured at different angles and as function of temperature could help us to identify the different reversal modes that take place at different temperatures and understand better the complexity of the low temperature effects.

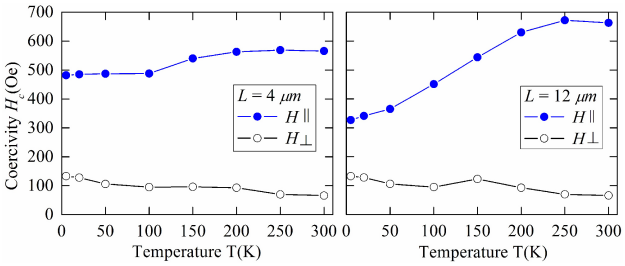

FIGURE 4. (lines) Temperature dependence of the coercivity for Ni nanowire arrays with length of L = 4 μm and L = 12 μm measured parallel and perpendicular to the nanowire axis. Both samples have same diameter d = 50 nm and lattice constant D = 100 nm.

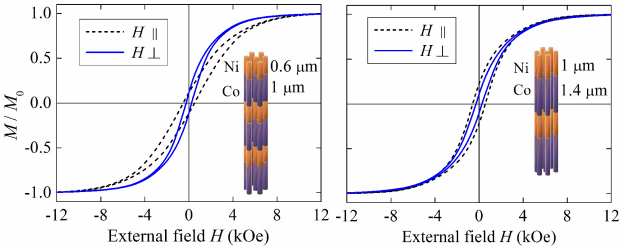

FIGURE 5. Hysteresis curves for Ni/Co segmented nanowire arrays, at different aspect ratios of the segments.

3.2. Hysteresis loops of segmented Ni/Co nanowire arrays

Figure 5 shows the hysteresis loops at 300 K for two segmented Ni/Co nanowire arrays electrodeposited in alumina membranes, both samples have same diameter d = 50 nm and lattice constant D = 100 nm. This Figure shows that the magnetic anisotropy can be adjusted alternating the magnetic material in different proportions of the segments.

4. Conclusions

Highly ordered nanowire arrays with different lengths and diameters of nanowires, were successfully fabricated by electrochemical deposition in alumina template with pore diameter d = 50nm and 60 nm, and interpore distance D = 100 nm. The electrodeposition potential also was varied in order to observe the influence of these parameters on the magnetic properties of the arrays. The increase of length of the nanowires result in the increase of the coercivity and remanence for all

diameters and the electrodeposition potentials studied here. By means of analytical calculations we have investigated the dependence of the coercivity as a function of the length and diameter of the nanowires. A good agreement between experimental and theoretical results is obtained. In conclusion, in nanowire arrays the magnetic anisotropy is dependent of the electrodeposition potential, temperature, length and diameter of nanowires. Therefore, the magnetic properties of interest (coercivity and remanence) can be adjusted by controlling these parameters and composition of nanowires (alternating the magnetic composition of nanowires).

Acknowledgements

This work was supported by the Proyecto Fondecyt Postdoctorado (Grant No. 3100117), and the Fondecyt (Grant Nos. 1080164 and 3080058).

1. R.P. Cowburn, D.K. Koltsov, A.O. Adeyeye, M.E. Welland, and D.M. Tricker, *Phys. Rev. Lett*. **83** (1999) 1042.
2. T. Gerrits, H.A.M. van den Berg, J. Hohlfeld, L. Bär, and Th. Rasing, *Nature* **418** (2002) 509.
3. R.H. Koch, J.G. Deak, D.W. Abraham, P.L. Trouilloud, R.A. Altman, Y. Lu, W.J. Gallagher, R. E. Scheuerlein, K.P. Roche, and S.S.P. Parkin, *Phys. Rev. Lett.* **81** (1998) 4512.
4. H. Masuda and K. Fukuda, *Science* **268** (1995) 1466.
5. J. Escrig, D. Altbir, M. Jaafar, D. Navas, A. Asenjo, and M. Vázquez, *Phys. Rev. B* **75** (2007) 184429.
6. M. Liu, J. Lagdani, H. Imrane, C. Pettiford, J. Lou, S. Yoon, V.G. Harris, C. Vittoria, and N.X. Sun, *Appl. Phys. Lett.* **90** (2007) 103105.
7. Z.K. Wang, H.S. Lim, V.L. Zhang, J.L. Goh, S.C. Ng, M.H. Kuok, H.L. Su, and S.L. Tang, *Nano Lett.* **6** (2006) 1083.
8. C.A. Ross, M. Hwang, M. Shima, J.Y. Cheng, M. Farhoud, T.A. Savas, H. I. Smith, W. Schwarzacher, F.M. Ross, M. Redjdal, and F.B. Humphrey, *Phys. Rev. B* **65** (2002) 144417.
9. P. Landeros, J. Escrig, D. Altbir, D. Laroze, J. d'Albuquerque e Castro, and P. Vargas, *Phys. Rev. B* **71** (2005) 094435.
10. M. Kröll, W.J. Blau, D. Grandjean, R.E. Benfield, F. Luis, P.M. Paulus, and L.J. de Jongh, *J. Magn. Magn. Mater.* **249** (2002) 241.
11. H. Foster, T. Schrefl, D. Suess, W. Scholz, V. Tsiantos, R. Dittrich, and J. Fidler, *J. Appl. Phys.* **91** (2002) 6914.
12. J. Escrig, R. Lavín, J.L. Palma, J.C. Denardin, D. Altbir, A. Cortés, and H. Gómez, *Nanotechnology* **19** (2008) 075713.
13. R. Hertel, *J. Appl. Phys.* **90** (2001) 5752.
14. R. Lavín, J.C. Denardin, J. Escrig, D. Altbir, A. Cortés, and H. Gómez, *IEEE Trans. Magn.* **44** (2008) 2808.
15. R. Inguanta, S. Piazza, and C. Sunseri, *Electrochim. Acta* **53** (2006) 5766.
16. G.C. Han, B.Y. Zong, P. Luo, and Y.H. Wu, *J. Appl. Phys.* **93** (2003) 9202.
17. A. Cortés, G. Riveros, J.L. Palma, J.C. Denardin, R. E. Marotti, E.A. Dalchiele, and H. Gómez, *J. Nanosci. Nanotechnol.* **9** (2009) 1992.
18. A. Kumar, S. Fahler, H. Schlorb, K. Leistner, and L. Schultz, *Phys. Rev. B* **73** (2006) 064421.
19. E.L. Silva, W.C. Nunes, M. Knobel, J.C. Denardin, D. Zanchet, K. Pirota, D. Navas, and M. Vázquez, *Physica B* **384** (2006) 22.
20. R. Hertel, *J. Magn. Magn. Mater.* **249** (2002) 251.
21. H. Forster, T. Schrefl, W. Scholz, D. Suess, V. Tsiantos, and J. Fidler, *J. Magn. Magn. Mater.* **249** (2002) 181.
22. P. Landeros, S. Allende, J. Escrig, E. Salcedo, D. Altbir, and E. E. Vogel, *Appl. Phys. Lett.* **90** (2007) 102501.
23. R. Lavin, J.C. Denardin, A.P. Espejo, A. Cortés, and H. Gómez, *J. Appl. Phys.* **107** (2010) 09B504.
24. D. Navas, PhD Thesis Universidad Autónoma de Madrid (2006).